Resonance Raman spectroscopy and quantum chemical modeling studies of protein-astaxanthin interactions in alpha-crustacyanin (major blue carotenoprotein complex in carapace of lobster, Homarus gammarus)

Weesie, R.J.; Merlin, J.C.; Lugtenburg, J.; Britton, G.; Groot, H.J.M. de; Jansen, F.J.H.M.; Cornard, J.P.

Resonance Raman Spectroscopy and Quantum Chemical Modeling Studies of Protein–Astaxanthin Interactions in α-Crustacyanin (Major Blue Carotenoprotein Complex in Carapace of Lobster, *Homarus gammarus*)

R. J. WEESIE,[1–3]* **J. C. MERLIN,[1]** **H. J. M. DE GROOT,[2]** **G. BRITTON,[3]** **J. LUGTENBURG,[2]** **F. J. H. M. JANSEN,[2]** **J. P. CORNARD[1]**

[1] Laboratoire de Spectrochimie Infrarouge et Raman, CNRS UMR 8516, Université des Sciences et Technologies de Lille, Bâtiment C5, 59655 Villeneuve d'Ascq CEDEX, France

[2] Leiden Institute of Chemistry, Gorlaeus Laboratories, Leiden University, P.O. Box 9502, 2300 RA Leiden, The Netherlands

[3] School of Biological Sciences, University of Liverpool, Crown Street, Liverpool L69 7ZB, United Kingdom

ABSTRACT: Resonance Raman spectroscopy and quantum chemical calculations were used to investigate the molecular origin of the large redshift assumed by the electronic absorption spectrum of astaxanthin in α-crustacyanin, the major blue carotenoprotein from the carapace of the lobster, *Homarus gammarus*. Resonance Raman spectra of α-crustacyanin reconstituted with specifically ^{13}C-labeled astaxanthins at the positions 15, 15,15′, 14,14′, 13,13′, 12,12′, or 20,20′ were recorded. This approach enabled us to obtain information about the effect of the ligand–protein interactions on the geometry of the astaxanthin chromophore in the ground electronic state. The magnitude of the downshifts of the C≡C stretching modes for each labeled compound indicate that the main perturbation on the central part of the polyene chain is not homogeneous. In addition, changes in the 1250–1400 cm^{-1} spectral range indicate that the geometry of the astaxanthin polyene chain is moderately changed upon binding to the protein. Semiempirical quantum chemical modeling studies (Austin method 1) show that the geometry change cannot be solely responsible for the bathochromic shift from 480 to 632 nm of protein-bound astaxanthin. The calculations are consistent with a polarization mechanism that involves the protonation or another interaction with a positive ionic species of comparable magnitude with both ketofunctionalities of the astaxanthin-chromophore and support the changes observed in the resonance Raman and visible absorption spectra. The results are in good agreement with the conclusions that were drawn on the basis of a study of the charge densities in the chromophore in α-crustacyanin by solid-state NMR spectroscopy. From the results the dramatic bathochromic shift can be explained not only from a change in the ground electronic state conformation but also from an interaction in the excited electronic state that significantly decreases the energy of the π-antibonding C≡O orbitals and the HOMO–LUMO gap. © 1999 John Wiley & Sons, Inc. Biospectroscopy 5: 358–370, 1999

Keywords: α-crustacyanin; astaxanthin; semiempirical calculation; electronic absorption; resonance Raman

INTRODUCTION

Carotenoids occur widely throughout the plant and animal kingdom and are responsible for many natural yellow, orange, or red colors. These colors may be modified when the carotenoid binds to a protein and forms a carotenoprotein complex. Striking examples of this phenomenon can be found among the blue-purple carotenoproteins that are present in marine invertebrate animals. Without a doubt the most extensively studied carotenoprotein complex is α-crustacyanin, the 320-kDa astaxanthin–protein from the carapace of the lobster, *Homarus gammarus*.[1] Natural α-crustacyanin consists of eight β-crustacyanin dimers (41 kDa), each of which contains two apoprotein subunits and two astaxanthin molecules. The astaxanthins are noncovalently bound to the apoproteins in a stoichiometric way. Upon binding of astaxanthin the wavelength of maximum absorption in the electronic absorption spectrum exhibits a dramatic shift from about 480 to 632 nm for protein-bound astaxanthin. The origin of this bathochromic shift, which is among the largest known in nature, has not been adequately explained, although several mechanisms have been proposed (see Zagalsky et al.[2] review). Buchwald and Jencks[3] suggested a distortion mechanism in which twisting about the double bonds of the conjugated polyene chain of astaxanthin was thought to occur. However, Salares et al.[4] rejected the distortion mechanism on the basis of their studies of the crustacyanins by resonance Raman (RR) spectroscopy. They favored a polarization mechanism in which the protein environment induces a charge redistribution of the π-electron system of the polyene chain. Elucidation of the underlying mechanism of such specific protein–chromophore interactions can contribute to the general level of understanding of receptor–acceptor interactions that play such an important role in many biological and biochemical processes.

The first direct experimental evidence for a charge redistribution mechanism was recently provided by solid-state ^{13}C-magic angle spinning (MAS) NMR spectroscopy.[5,6] In these studies specifically ^{13}C-labeled astaxanthins were synthesized, reconstituted into the protein complex, and subsequently studied by ^{13}C-MAS NMR. The successes of ^{13}C-MAS NMR in combination with site-specific isotopic labeling to study atomic charge density variations due to protein–chromophore interactions instigated a complementary RR study into the vibrational structure of the α-crustacyanin complex reconstituted with specifically ^{13}C-labeled astaxanthins. Previous studies[1] indicated that the C(20) and C(20′) methyl groups are involved in steric interactions necessary for binding. The nature of these interactions could not be resolved with the cross polarization (CP)-MAS techniques. To probe the central part of the chromophore in more detail, we present the first RR spectra of α-crustacyanin reconstituted with [15]-, [15,15′]-, [14,14′]-, [13,13′]-, [12,12′]-, or [20,20′]-^{13}C astaxanthin (Fig. 1).

A qualitative assignment of the vibrational bands of free astaxanthin based on the resonance and FT-Raman spectra of these differently labeled astaxanthins was presented in a previous publication.[7] Here we focus on the effects of protein binding on the structural properties of the astaxanthin molecule by probing the differences in spectral features in the RR spectra of the free and protein-bound astaxanthins. In addition, the Raman data are correlated with the results of quantum chemical calculations of the ground-state geometry of several electrostatically perturbed astaxanthins. An analysis of the differences between the geometrical parameters of astaxanthin and these astaxanthin-like structures compared with the spectral differences of free astaxanthin and α-crustacyanin enabled us to exclude or favor certain models for protein-bound astaxanthin.
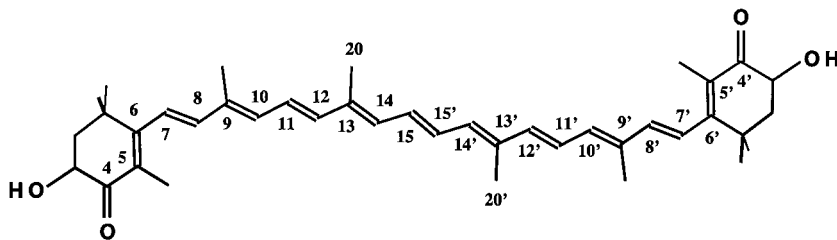

Figure 1.   The chemical structure of astaxanthin (3,3′-dihydroxy-β,β-carotene-4,4′-dione) and atom numbering.

MATERIALS AND METHODS

Extraction and Purification of α-Crustacyanin

The α-crustacyanin was extracted from finely ground lobster carapace and subsequently purified by anion-exchange and gel-filtration chromatography as previously described.[8] The extraction and purification stages were all carried out at 4°C and the pH was maintained at between 6.5 and 7.5.

The purity of the α-crustacyanin preparation was checked after each purification step by measuring the ratio of the absorbance at 632 nm to the protein absorbance at 280 nm, and the total amount of α-crustacyanin present in the protein solution was determined from the absorbance at 632 nm. A molar absorption coefficient ($\varepsilon = 1.25 \times 10^5 \; M^{-1}cm^{-1}$) was used.[9]

Reconstitution of α-Crustacyanin with ^{13}C-Labeled Astaxanthins

The organic synthesis of the ^{13}C-labeled astaxanthins is described elsewhere.[10] The reconstitution procedure was based on a method presented in an earlier study.[8] All stages of reconstitution were carried out at 0°C in a ground glass stoppered tube; any solvents or buffers added during the procedure were first cooled to 0°C. Acetone was added quickly with much stirring to the α-crustacyanin in 50 mM sodium phosphate buffer (pH 7.0, 2 mL, containing up to 3 mg protein), followed immediately by the addition of diethyl ether (10 mL). The tube was inverted 3 times and the orange ether layer containing extracted astaxanthin was pipetted off after the two phases separated. Ether was added and pipetted off twice until no more carotenoid could be extracted. Any remaining ether was quickly removed with a gentle flow of nitrogen and the protein solution was made up to 2 mL again with 50 mM sodium phosphate buffer (pH 7.0) if necessary. The acetone and ether extraction was repeated 2 more times, removing virtually all the astaxanthin and leaving an almost transparent apoprotein preparation. Finally all the volatile solvent remaining was removed with a nitrogen flow during 5–10 min.

A 25% molar excess of the ^{13}C-labeled astaxanthin in acetone (1.25 mL) was quickly added to the apoprotein preparation with much stirring, followed immediately by the addition of 50 mM sodium phosphate buffer (pH 7.0, 10 mL). This mixture was dialyzed for 18 h against 5 L of the same buffer. The reconstituted complex was shown to be identical to the natural α-crustacyanin as judged by the electronic absorption, RR, and ^{13}C-CP-MAS NMR spectra of both species.[5]

RR Spectroscopy

The RR spectra of the α-crustacyanins were recorded with a DILOR RTI spectrometer and the excitation was provided by a Spectra-Physics 2000 Kr^+ laser (647.1 nm) or a Spectra-Physics Ar^+ laser (488.0 nm). A typical output power of 50–100 mW was used, which was reduced to approximately 5 mW when the laser beam reached the sample. The slit bandwidth was set to 4–6 cm^{-1} and the spectrometer was calibrated using the laser plasma lines, yielding an accuracy of at least 2 cm^{-1}.

All RR spectra were recorded at room temperature. To exclude possible photodecomposition of astaxanthin and the α-crustacyanin, the rotating cell technique was used. In all cases the reproducibility of the spectral features was verified as a function of both the irradiation time and the laser power. The spectra of the α-crustacyanin were obtained in 50 mM phosphate buffer, and a typical sample volume of about 3 mL with an optical density of approximately 0.2 at the wavelength of maximum absorbance was used.

Computational Methods

Geometry optimizations of astaxanthin and of the different astaxanthin-like structures were performed with a combination of classical molecular mechanics and semiempirical quantum chemical methods. The initial configurations were set up with standard geometrical parameters that were subsequently optimized using the MMX force field, including the π-VESCF calculations in the PC model (version 3.2) program package.[11] The refined structures were then used as input data for geometry optimizations by the Austin method 1 (AM1)[12] using the HYPERCHEM package (version 4.5)[13] on a Pentium microcomputer. Calculations on the electrostatically perturbed astaxanthin-like structures were performed using the geometrical parameters of the optimized astaxanthin molecule as input data. The energy minimization was carried out with the Polak–Ribiere algorithm using a convergence criterion of 0.005 kcal mol^{-1}. For the calculation of the electronic absorption spectrum, a limited configuration in-

teraction (CI) treatment was used that was based on a 11×11 CI matrix. Only the contributions of the singly excited configurations were considered.

RESULTS AND DISCUSSION

RR Spectroscopy of α-Crustacyanins

Although RR spectroscopy has been used extensively to study protein–chromophore interactions in carotenoproteins,[4,9,14–18] the use of specifically isotopically labeled chromophores in these investigations is completely new. It requires the synthesis of isotopically enriched carotenoids and subsequent incorporation into the carotenoprotein complex.[8,10] In this work the protein–chromophore interactions in α-crustacyanin were studied using specifically[13]C-labeled astaxanthins. Previous Raman experiments suggested that the central part of the astaxanthin chromophore is in a relatively planar conformation and only slightly distorted.[14] In contrast, inferences from reconstitution experiments with demethylated astaxanthins[19,20] and the distortion mechanism proposed by Buchwald and Jencks[3] favor a more twisted conformation. These conflicting opinions made us decide to start with the investigation of the central part of the chromophore and to study the effects upon protein binding on the vibrational frequencies in this particular region.

The RR spectra of [15-^{13}C]-, [15,15′-^{13}C]-, [14,14′-^{13}C]-, [13,13′-^{13}C]-, [12,12′-^{13}C]-, and [20,20′-^{13}C]-astaxanthin in CCl_4 solution and bound to the α-crustacyanin complex are presented in Figures 2 and 3, respectively. The spectra of the free astaxanthins and the effects that were observed due to the replacement of a ^{12}C by a ^{13}C isotope were extensively discussed in a previous publication.[7] The assignment of these Raman bands to vibrational modes, which result from excitation into the π–π^* transition of the conjugated polyene chain, is well established.[7] Here we focus on astaxanthin bound to α-crustacyanin in order to obtain information about the nature of the binding mechanism and the architecture of the astaxanthin binding site on the basis of the spectra of the different protein-bound astaxanthins. As previously observed, all spectra of free astaxanthin in CCl_4 are characterized by three intense bands that occur at 1523, 1159, and 1008 cm^{-1} in the RR spectrum. The intensities in the RR spectrum are determined by the slope of
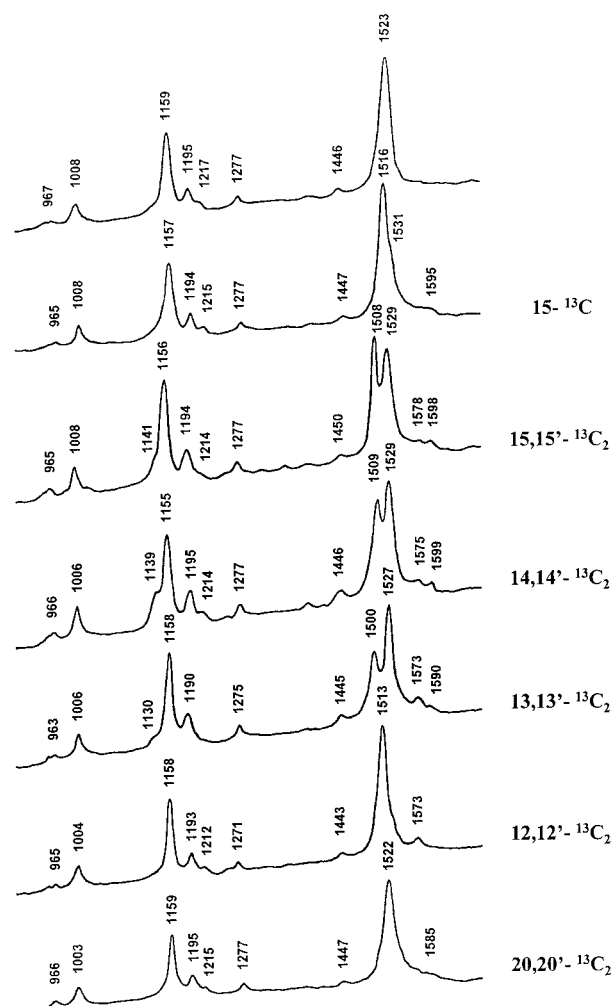

Figure 2. Resonance Raman spectra of (top to bottom) natural astaxanthin, [15-^{13}C]-, [15,15′-^{13}C$_2$]-, [14,14′-^{13}C$_2$]-, [13,13′-^{13}C$_2$]-, [12,12′-^{13}C$_2$]-, and [20,20′-^{13}C$_2$]-astaxanthin in CCl_4. Spectra were recorded at room temperature and an excitation wavelength ($\lambda_{exc.}$) of 488 nm was used.

the multidimensional potential energy surface in the Franck–Condon region. For a polyene the predominant excited state evolution is along the modes describing the bond order rearrangement of the polyene and modes that have a significant projection onto these displacements. Hence, the most intense band at 1523 cm^{-1} (ν_1 line) is assigned to the C=C stretch vibrations of the polyene chain with a significant contribution of the C(11)=C(12), C(13)=C(14), C(14′)=C(13′), and C(12′)=C(11′) in-phase stretches, confirming the normal mode calculations performed by Saito and Tasumi[21] and the study of labeled astaxanthins.[7] The C(15)=C(15′) stretch is expected at higher
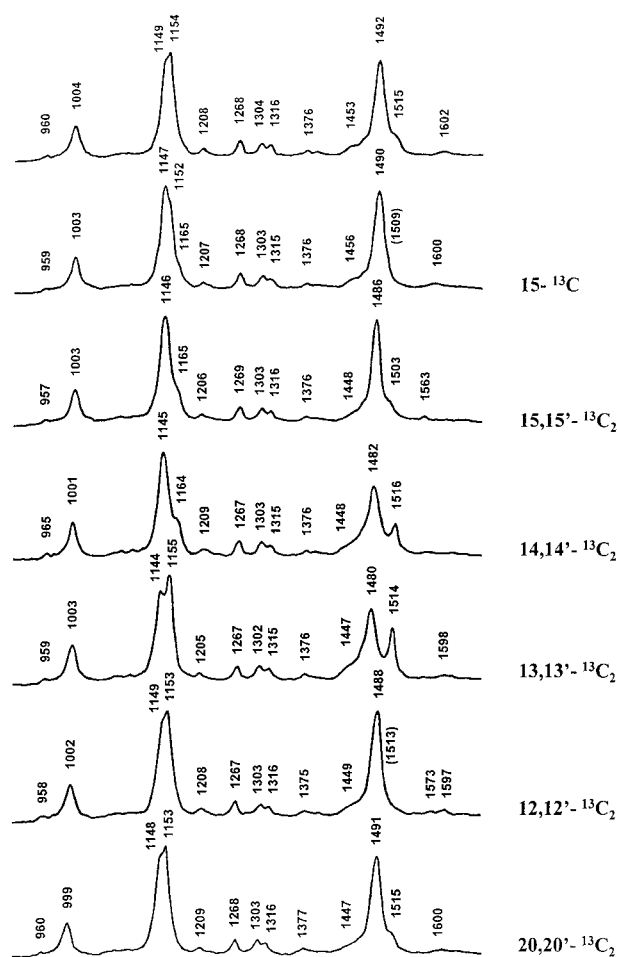
Figure 3. Resonance Raman spectra of (top to bottom) natural α-crustacyanin and α-crustacyanin reconstituted with [15-^{13}C], [15,15′-^{13}C$_2$], [14,14′-^{13}C$_2$], [13,13′-^{13}C$_2$], [12,12′-^{13}C$_2$], and [20,20′-^{13}C$_2$]-astaxanthin in phosphate buffer solution (pH 7.0). Spectra were recorded at room temperature and an excitation wavelength (λ_{exc}) of 647.1 nm was used. (*) The position of lines observed only with a blue excitation (488 nm).

frequency. The second most intense band at 1159 cm^{-1}, which is also referred to as the ν_2 line, is in fact the superposition of two modes that can be ascribed to C—H in-plane bending vibrations mixed with C—C stretching and C=C—C bending vibrations, respectively. The third intense line (ν_3) at 1008 cm^{-1} can be assigned to CH$_3$ in-plane rocking vibrations.

Upon binding to α-crustacyanin the Raman spectrum of astaxanthin is changed. Bands are shifted, intensity is redistributed, and new lines appear, in particular in the "fingerprint" region between 1250 and 1400 cm^{-1}. The ν_1 line of pro-

tein-bound astaxanthin shifts from 1523 to 1492 cm^{-1} and its intensity, relative to that of the ν_2 and ν_3 lines, diminishes. The 31 cm^{-1} downshift is in good agreement with the bathochromic shift of the wavelength of maximum light absorption (λ_{max}). An empirical relationship was established by Rimai et al.[22] for polyenes of increasing chain length and was taken to reflect the extent of π-electron delocalization along the polyenic chain for a number of carotenoids in a given solvent. For some astaxanthin containing proteins[4,15,17] a new kind of correlation associates the decreasing energy gap between the ground electronic and excited states ($\sim 1/\lambda_{max}$) with the decrease in the ν_1 wavenumber, which remains a property of the electronic ground state only. The downshift of the ν_1 line in α-crustacyanin provides unambiguous evidence that increased π-electron delocalization for complexes in the ground electronic state is a contributing factor to the spectral characteristics. However, the change of the intensity ratios between the ν_1, ν_2, and ν_3 response shows that the excited state is also affected. This implies that the exciton model in which astaxanthins are arranged in a head to tail stacking cannot be considered as a predominant mechanism responsible for the bathochromic shift. Although it was shown that such a stacking would give rise to a red shift of the absorption maximum,[14,23] it would involve a major perturbation of mainly the electronic excited state of astaxanthin, which was excluded by our experiments.

A distinct shoulder enhanced by a green or blue excitation was observed on the high-frequency side of the ν_1 line. This line, which was previously assigned either to partly denatured carotenoprotein or to the presence of different binding sites[4] in the protein, was in fact observed for all the ^{13}C-labeled astaxanthins. For [14,14′-^{13}C] and [13,13′-^{13}C] there was a significant intensity after excitation with a blue line (488 nm) and a shoulder was observed for [15,15′-^{13}C] and [20,20′-^{13}C]. For [15-^{13}C] and [12,12′-^{13}C] reconstituted α-crustacyanin it was only observed with a blue excitation of 488 nm.

The shifts upon protein binding for the specifically ^{13}C-labeled astaxanthins may reveal information about the effects of the surrounding apoprotein on a localized mode. In order to quantify these effects, the spectral shifts of the ν_1 modes for free and protein-bound astaxanthins are presented in Table I. It is noted that the frequency shifts upon ^{13}C labeling (named Δ^{13}C) are significantly different when comparing α-crustacyanin

Table I. Vibrational Wavenumbers (cm^{-1}) for ν_1, ν_2, and ν_3 Lines of Free and Protein-Bound Astaxanthins

| | ν_1 Line | | | | | ν_2 Line | | | ν_3 Line | | |
| | Free | | Bound | | | | Bound | | | Bound | |
		Δ^{13}C		Δ^{13}C	Δ	Free		Δ	Free		Δ
Natural astaxanthin	1523		1492		−31	1159	1149	−10	1008	1004	−4
			1515 (sh)				1154	−5			
[15]-^{13}C	1516	−7	1490	−2	−26	1157	1147	−10	1008	1003	−5
	1531 (sh)		(1509)	−6			1152	−5			
							1165 (sh)				
[15,15′]-^{13}C	1508	−15	1486	−6	−22	1156	1146	−10	1008	1004	−4
	1529		1504 (sh)	−11			1165 (sh)				
[14,14′]-^{13}C	1509	−14	1482	−10	−27	1155	1145	−10	1006	1001	−5
	1529		1516	+1	−13		1164				
[13,13′]-^{13}C	1500	−23	1480	−12	−20	1158	1144	−14	1006	1003	−3
	1527		1514	−1	−13		1155	−3			
[12,12′]-^{13}C	1513	−10	1488	−4	−25	1158	1149	−9	1004	1002	−2
			(1513)	−2			1153	−5			
[20,20′]-^{13}C	1522	−1	1491	−1	−31	1159	1148	−11	1003	999	−4
			1517 (sh)	+2			1153	−6			

The Δ^{13}C indicates the shift upon ^{13}C labeling and Δ indicates the shift upon binding on crustacyanin. The wavenumbers in parentheses are observed only with a blue excitation.

with free astaxanthins, indicating that the degree of mixing of the C=C stretch vibrations in the ν_1 spectral range is changed upon protein binding.

The spectrum of α-crustacyanin reconstituted with [20,20′-^{13}C]-astaxanthin is similar in wavenumber and relative intensities to that of unlabeled α-crustacyanin. This illustrates that the ground and excited state spectral features are mainly determined by the polyenic chain. Assuming that the C=C stretch vibrations are shared between two bands for all the investigated compounds, we can consider that the 1492 cm^{-1} line contains a significant contribution of C(13)=C(14) and C(13′)=C(14′) stretches. Indeed, the low-frequency component of the ν_1 mode is shifted by 10 and 12 cm^{-1} in the spectra of α-crustacyanin reconstituted with [14,14′-^{13}C]- and [13,13′-^{13}C]-astaxanthin, respectively, whereas the shifts of the low-frequency components of [15-^{13}C]-, [15,15′-^{13}C]-, and [12,12′-^{13}C]-astaxanthin only amount to 2, 6, and 4 cm^{-1}, respectively, compared to natural α-crustacyanin. The high-frequency component in the spectra of

crustacyanin reconstructed with [15-^{13}C]- and [15,15′-^{13}C]-astaxanthin is subjected to significant downshifts of 6 and 11 cm^{-1} when compared to natural α-crustacyanin, indicating that the distinct shoulder observed for all the investigated compounds contains a significant contribution of C(15)=C(15′) stretch. Because the observed ^{13}C shift for a given line is strongly dependent on the potential energy distribution of the normal modes, it is difficult to draw a direct conclusion from the shifts obtained upon the complexation of astaxanthin by the apoprotein. However, if we consider the spectra of [14,14′-^{13}C]-astaxanthin, the ^{13}C shifts of similar magnitude for free and bound molecules (14 and 10 cm^{-1}, respectively) led us to consider that the contribution of C(13)=C(14) and C(14′)=C(13′) stretches are comparable for the low-frequency component. In the spectra with [14,14′-^{13}C]-astaxanthin this component is considerably downshifted by 27 cm^{-1} in α-crustacyanin while the shift of the high-frequency component, which is expected to contain a significant contribution of C(15)=C(15′)

stretch, only amounts to 13 cm^{-1}. This suggest that the outer C(13)=C(14) and C(14$'$)=C(13$'$) bonds could be more perturbed than the central C(15)=C(15$'$) bonds. Support for this comes from the observation that the low intensity Raman bands between 1550 and 1600 cm^{-1} that are observed in the spectra of astaxanthin and that can be assigned to the terminal C=C stretch vibrations disappeared in the spectra of α-crustacyanin. The vibration frequencies of the terminal C=C stretch are decreased and may contribute to the high-frequency component of the ν_1 line. This would be in good agreement with the conclusions that were obtained on the basis of solid-state MAS NMR, which strongly favor a protonation of both ketofunctionalities of astaxanthin.[6,24] Quantum chemical calculations show that such a protonation mechanism would have the greatest effect both in terms of electronic charge density and geometrical parameters on the outer part of the astaxanthin polyene chain. Moreover, in all labeled and nonlabeled α-crustacyanin spectra a small line appears near 1600 cm^{-1} (see Fig. 3). The value of it is too high to assign this line to a terminal C=C stretch mode, and a carbonyl stretch mode enhanced by this change in electronic charge density on the outer part of the astaxanthin molecule can be proposed. The downshift of 50 cm^{-1}, which was compared to the value observed in the free astaxanthin spectrum in an off-resonance condition,[7] can be related to the protonation of this function. The appearance of this line should indicate the participation of the C=O groups in the blue chromophore.

The enhancement of the low-frequency component of the ν_1 line in the spectra of α-crustacyanins reconstituted with [15,15$'$-^{13}C]-, [14,14$'$-^{13}C]-, and [13,13$'$-^{13}C]-astaxanthin is more important than that observed in the spectra of the free labeled analogues. Because normal modes can change their internal coordinate character upon electronic excitation, it is too hazardous to draw a conclusion.

The ν_2 line of α-crustacyanin is split in two separate components at 1149 and 1154 cm^{-1}. The higher component, which disappears in the spectra of α-crustacyanin reconstituted with [15-^{13}C]- and [15,15$'$-^{13}C]-astaxanthin, can be assigned to a mode containing a significant amount of C(14)—C(15) and C(15$'$)—C(14$'$) stretch vibrations. The lower component is not significantly affected by ^{13}C substitution and can be assigned to a C—H bending mode. The observation of two overlapping modes is consistent with our previous assignment of the ν_2 line of astaxanthin.[7] An additional feature is formed by the appearance of lines at 1165, 1165, and 1164 cm^{-1} in the spectra of α-crustacyanin reconstituted with [15-^{13}C]-, [15,15$'$-^{13}C]-, and [14,14$'$-^{13}C]-astaxanthin, respectively, but we can easily assume that this line, which is already present in the spectrum of α-crustacyanin, can be revealed only by the downshift of the 1159 cm^{-1} component. If the electronic delocalization of the π-electron system upon protein binding is increased by a polarization mechanism from the terminal regions, it should be accompanied by an increase of nonbonding character and yield a lengthening of the polyene carbon skeleton bonds. This is expected to be expressed in a downshift of the ν_1 line (as observed) and an upward shift of the ν_2 line. The fact that ν_2 exhibits the opposite behavior for carotenoids has never been fully understood. However, the low-frequency components observed at 1141 cm^{-1} in the FT-Raman spectrum of [15-^{13}C]-astaxanthin[7] and at 1141 and 1135 cm^{-1} in the RR spectra of [15,15$'$-^{13}C]- and [14,14$'$-^{13}C]-astaxanthin (Fig. 2), respectively, which can be assigned to shifted C(14)—C(15) and C(15$'$)—C(14$'$) stretches, provides a possible explanation for this conundrum. Because the coupling of these C—C modes with C—H bending modes is significantly decreased upon ^{13}C labeling, they can be observed separately. However, in natural α-crustacyanin this mode is hidden by the strong ν_2 line. Finally, the ν_3 line shifts approximately 4 cm^{-1} downward upon complexation and does not exhibit any significant differences for the different isotopic labels.

The spectra of the α-crustacyanins exhibit many resonance enhanced bands in the 1250–1400 cm^{-1} spectral region that are lacking in the spectra of the unbound astaxanthins. These lines are assigned to C—H in-plane bending vibrations that become Raman active for α-crustacyanin. The appearance of these lines strongly suggests that the geometry of the polyene chain is changed upon binding, because the projection of the ethylenic C—H bending modes is strongly enhanced by conformational and configurational distortions of the polyene. However, the changes in geometry should be small, and the absence of a hydrogen out of plane mode in the 800–950 cm^{-1} region argues against a large protein induced distortion of the central part of the polyene chain. In addition, the C—H bending modes are not very sensitive to ^{13}C substitution in the central part. The presence of some terminal ring modes in this

spectral range can be excluded by the recording of spectra of crustacyanins reconstituted with carotenoids with different terminal rings (data not shown) such as actinioerythrol (3,3'-dihydroxy-2,2'-dinor-β,β-carotene-4,4'-dione) and astacene (3,3'-dihydroxy-2,3,2',3'-tetradehydro-β,β-carotene-4,4'-dione). The high degree of similarity of this spectral range for all investigated complexes suggests that the conformation of the polyene chain in the protein binding pocket is independent of the nature of the terminal ring. We can notice also that for the complexes with astacene and actinioerythrol, which contain a keto group on the terminal rings, a small line assignable to a C=O stretching is also observed near 1600 cm^{-1} in the RR spectrum.

Semiempirical Quantum Chemical Modeling Studies

From optical spectroscopy data it was concluded that the astaxanthin bound to α-crustacyanin is spectroscopically a monomer.[3] Recent solid-state NMR and quantum chemical modeling data support a mechanism in which an additional electrostatic polarization of the chromophore is induced by binding to the protein. The electrostatic effects most likely originate from the keto groups in the β-ionone rings. It was shown that the main perturbation of astaxanthin upon binding to the protein has a symmetric character with similar effects on both halves of the molecule, while an additional smaller perturbation gives rise to small asymmetric effects in the charge redistribution pattern along the polyenic chain.[6,24]

The spectral shifts of the ground-state normal modes of astaxanthin that are observed upon protein binding provide additional information about the spatial and electronic structure of the astaxanthin–chromophore in the α-crustacyanin complex. In order to interpret these shifts and to correlate them with other available experimental data, semiempirical quantum chemical calculations were performed for free astaxanthin and for a single carotenoid molecule exposed to highly localized and specific interactions with pronounced charge effects on the polyene system.[6,24]

The present Raman data of α-crustacyanin reconstituted with different ^{13}C-labeled astaxanthins show that the delocalization of the astaxanthin polyene chain is increased upon protein binding and that the positive charge is increased, which is illustrated in a downward shift of the ν_1 line and a shift toward higher frequency of the
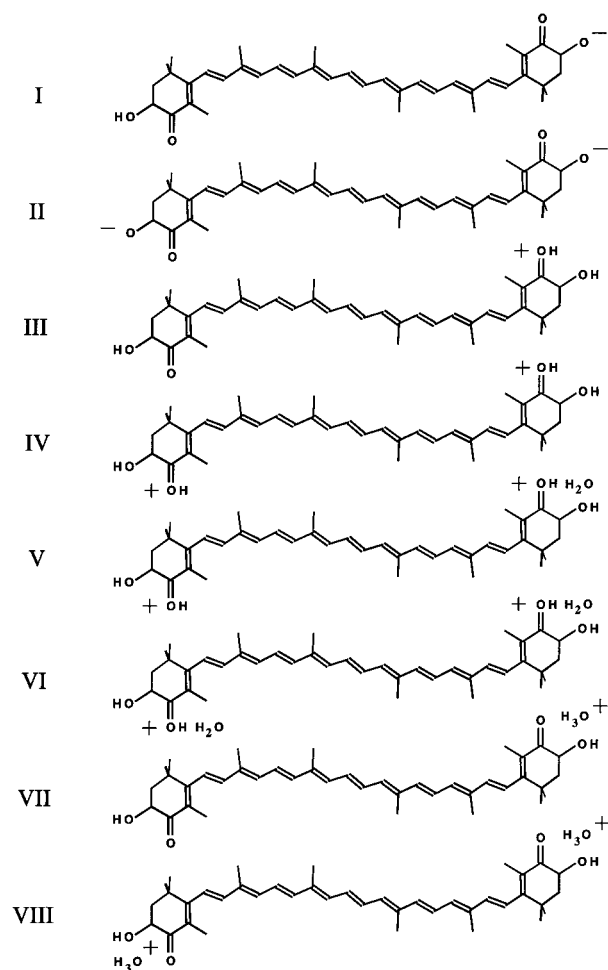

Figure 4. The chemical structures of the electrostatically perturbed astaxanthin molecules, which were assessed as possible models for protein-bound astaxanthin.

C—C stretch vibrations. This can be translated into a lengthening of the C=C bonds and a shortening of the C—C bond lengths. In this light, the optimized geometries of the different astaxanthin-like structures could help to investigate the validity of certain models for protein-bound astaxanthin. The astaxanthin-like structures shown in Figure 4 are all subjected to strong highly localized interactions that affect either the keto or hydroxy groups of the β rings. This is easily achieved in the virtual reality of the computer by having either one or both of the β-ring hydroxyl groups deprotonated (structures I and II) or by protonation of either one or both astaxanthin keto groups (structures III and IV), in which case the associated positive charge delocalized along the polyene chain can be stabilized
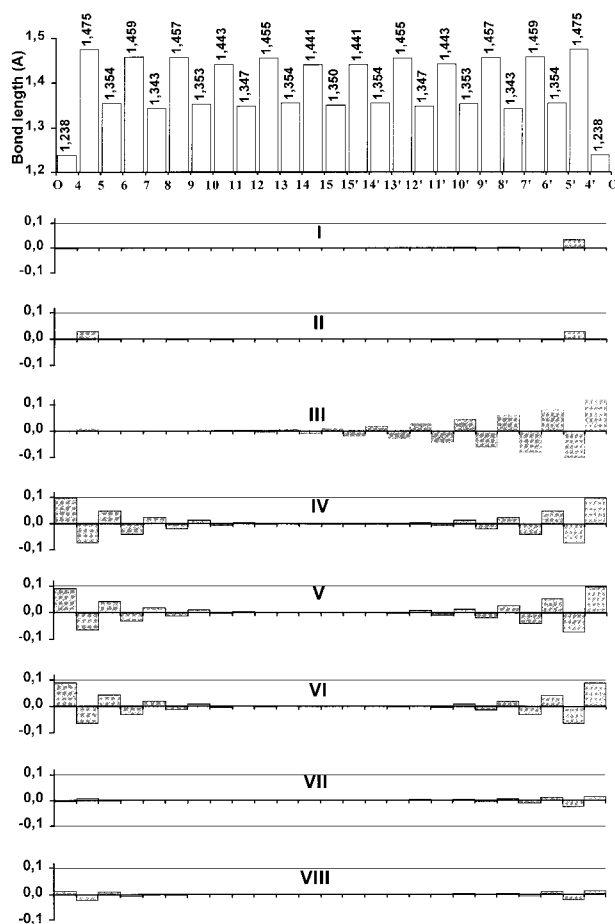
Figure 5. The calculated bond length of the polyenic chain of astaxanthin and the calculated bond length variation for the different forms of electrostatically perturbed astaxanthin molecules presented in Figure 4.

with a water molecule in a hydrogen bonding position (structures V and VI). Alternatively, an H_3O^+ ion can be positioned into a hydrogen bonding configuration with the keto groups (structures VII and VIII). Our AM1 calculation indicates that when one ion is initially positioned in the direct surrounding of the keto group in one β-ionon ring, a proton can migrate toward the oxygen atom to form a protonated keto group stabilized by a hydrogen bonded water molecule ($H_2O \cdot H—O═C$ = 2.06 Å). The calculated heat of formation of structure VI (ΔH = 106.43 kcal mol^{-1}) is significantly lower than that obtained for structure VIII (ΔH = 128.45 kcal mol^{-1}). The differences between the calculated bond length of astaxanthin and these electrostatically perturbed astaxanthin molecules are presented in Figure 5. At the Hartree–Fock level considered here, all models exhibit an increase in C═C bond lengths and a

decrease in C—C lengths in accordance with the expected increase of delocalization along the polyenic chain, although the magnitude of the calculated changes in bond length are not the same for the different models. The very low values for deprotonated (structures I and II) and hydrogen bonded hydroxonium ion (structures VII and VIII) molecules can justify the exclusion of these four structures as models of interaction. Only a protonation mechanism can be considered but, because the correlation between the degree of delocalization and geometrical parameters remains qualitative, no direct information can be obtained on the basis of this calculation. However, we can see that the protonation of a single keto group (structure III) can produce a perturbation that affects the middle of the chain [Δl = +0.013, +0.02, and +0.03 Å, respectively, for the $C(15)═C(15')$, $C(14')═C(13')$, and $C(12')═C(11')$ bonds]. Such an effect should produce a significant change in wavenumber in the ν_1 spectral range. The symmetric perturbation of the two keto groups (structure IV) led to a lower change: the Δl values for the three above-mentioned bonds are +0.001, +0.002, and +0.005 Å, respectively. The stabilization of one or two protonated keto groups by water molecules (structures V and VI) weakly reduces the changes in the bond length. However, we can notice that the position of the water molecule relative to the protonated group can polarize the charge and therefore modulate the bond alternation pattern in the polyenic chain. For the structure V, which is stabilized by only one water molecule, we obtain a small asymmetric perturbation of the bond length: the calculated Δl values for the three central double bonds are +0.001, +0.002, and +0.006 Å.

Assuming a linear relationship between bond length and the force constant (l = 1.54 Å, k = 4.4 mdyne Å^{-1} for a C—C bond and l = 1.35 Å, k = 9.1 mdyne Å^{-1} for a C═C bond),[25] the estimated shift for an isolated harmonic oscillator is close to 20 cm^{-1} for a change in the bond length of 0.005 Å. This value is in accordance with the shift observed in the RR spectra of α-crustacyanin. With this assumption the shift for the monoprotonated molecule is estimated to be in the range of 50–100 cm^{-1}, which is too high compared to the experimental data. The harmonic force constants and the frequencies of the vibrational normal modes of monoprotonated (III) and biprotonated (IV) forms of astaxanthin were performed from the equilibrium molecular geometry determined by the AM1 method. As previously determined for

Table II.   Experimental λ_{max} for Free and Bound Astaxanthin, and Calculated λ_{max} for Different Forms of Perturbed Astaxanthin Molecules Presented in Figure 4

| | Astaxanthin in CCl_4 | α-Crustacyanin in Phosphate Solution (pH 7.0) | Perturbed Astaxanthin Molecules | | | | | | | |
			I	II	III	IV	V	VI	VII	VIII
λ_{max} (nm)	446	632	458	444	767	629	619	599	484	477

astaxanthin,[7] this method gives only an approximate description of the vibrational normal modes and cannot be used for the assignment of individual normal modes. However, with the use of a suitable scaling factor (0.84), the spectral range for the C=C stretching modes was correctly predicted for astaxanthin. Considering the specific vibrational normal mode where all the C=C bonds in the C(11)—C(11′) fragment of the polyenic chain move in phase, the magnitude of the downshifts for structures III and IV, compared to the wavenumber calculated for astaxanthin, are 120 and 29 cm^{-1}, respectively. This indicates that, even if the self-consistent field mean field of the Hartree–Fock overestimates the bond order alternation, this semiquantitative analysis is consistent with the experimental data.

In order to assess the validity of the remaining models, electronic transition energies were calculated using the AM1 Hamiltonian in a CI calculation that included all singly excited state configurations from the 11 highest occupied orbitals to the 11 lowest unoccupied orbitals. For astaxanthin the HOMO–LUMO transition had the largest oscillator strength in the calculated electronic spectrum, corresponding to a λ_{max} of 446 nm that is close to the observed value of 480 nm in solution, particularly if one takes into account that the calculations are performed on a molecule *in vacuo*, neglecting the influence of solvent–carotenoid interactions. All the proposed interactions induce a red shift of the absorption maximum whose magnitude depends on the electronic polarizability of the solvent. Therefore, the calculated λ_{max} values are expected to be slightly lower than the experimental data, which supports the reliability of these criteria to evaluate the other astaxanthin-like structures as models for protein-bound astaxanthin. The calculated values for the different model structures are presented in Table II. They demonstrate that only a charging by protonation can induce spectral shifts that are of the order of the 150-nm bathochromic shift of astaxanthin upon protein binding. All the other mod-

els only undergo minor spectral shifts, which range from a hypsochromic shift of 2 nm for doubly deprotonated astaxanthin (structure II) to a bathochromic shift of 37 and 30 nm for hydroxonium ions hydrogen bonded with astaxanthin (structures VII and VIII). Of the protonated astaxanthin models the singly protonated astaxanthin (structure III) has a theoretical λ_{max} of 767 nm and the doubly protonated astaxanthin has its absorption maximum at 629 nm. Stabilization of the positive charge by one or two water molecules is responsible for a slight hypsochromic shift. The singly protonated astaxanthin model was already eliminated on the basis of the changes in bond length, which means that only doubly protonated astaxanthin (structure IV) withstands both criteria and can be proposed as a model for the astaxanthin–protein interactions that are responsible for the color shift of the blue carotenoprotein from the carapace of the lobster *Homarus gammarus*.

Furthermore, we noted that the calculated 629 nm is in very good agreement with the absorption maximum of 632 nm of α-crustacyanin if the deviation of the theoretical λ_{max} toward shorter wavelengths due to the lack of interactions with the surrounding medium is taken into account.[6] The λ_{max} values calculated for structures V and VI illustrate the influence of the interaction with surrounding molecules on the polarization of the polyenic chain. This result corroborates the correlation between ^{13}C-NMR chemical shifts and electronic charge densities.[6] Additional support for the protonation mechanism comes from the fact that despite extensive explorations with the semiempirical quantum chemical methods, no other astaxanthin-like structure that exhibited a red shift similar to α-crustacyanin was found. In particular, a structure that involved twisting around the double bonds of the polyenic chain, as envisaged in the model of Buchwald and Jencks,[3] only yielded a moderate bathochromic shift. Therefore, we can exclude the distortion mechanism as being the sole mechanism responsible for

LUMO+1   - 0.85 eV
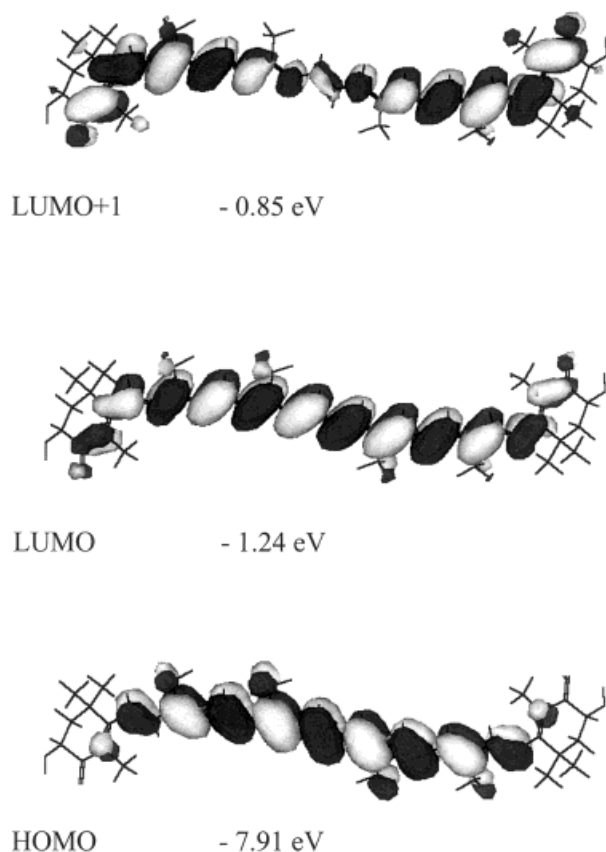
LUMO   - 1.24 eV

HOMO   - 7.91 eV

Figure 6. A schematic representation of the orbitals involved in the optical transition of astaxanthin.

the bathochromic shift of protein-bound astaxanthin. Other structures like a dienol and dienolate forms or astaxanthin in which the hydrogens have migrated from the hydroxyl groups to the keto groups were also considered, but the calculated λ_{max} values reject these hypotheses.[6]

The CI calculation performed on the astaxanthin molecule[7] indicates that mainly the HOMO → LUMO configuration (with a CI coefficient of 0.58) is involved in the strong visible transition calculated at 446 nm (observed at 468 nm in petroleum ether[7]). A schematic representation of the geometry of the two involved orbitals (Fig. 6) indicates the π–π* character of the optical transition. For the doubly protonated astaxanthin (structure IV) the CI calculation indicates that the transition with the largest oscillator strength in the visible range is a mixing of the HOMO → LUMO and the HOMO-1 → LUMO+1 configurations with respective CI coefficients of 0.418 and 0.348. As illustrated in Figure 7, in the LUMO and the LUMO+1 representation the contribution of the antibonding C=C orbitals of the poly-

enic chain is less important than in astaxanthin and a significant participation of the C=O antibonding orbitals is observed. The geometry of the LUMO+2 for the doubly protonated molecule (Fig. 6) is similar in shape to the LUMO calculated for astaxanthin (Fig. 7), and the geometry of the HOMOs are rather similar for astaxanthin and doubly protonated astaxanthin. In others words, two nearly degenerate orbitals (not observed for pure astaxanthin) appear in the middle of the π–π* gap for the biprotonated species. The participation of the C=O antibonding character in astaxanthin is observed in a great number of

LUMO+2   - 4.78 eV

LUMO+1   - 6.32 eV

LUMO   - 6.36 eV

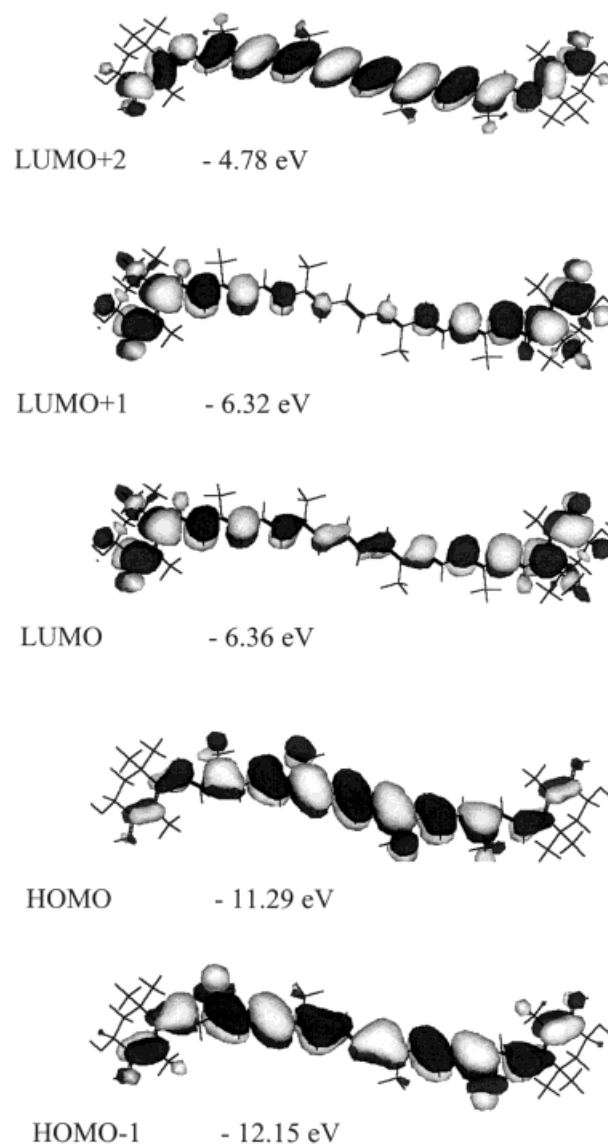HOMO   - 11.29 eV

HOMO-1   - 12.15 eV

Figure 7. A schematic representation of the orbitals involved in the optical transition of doubly protonated astaxanthin (structure IV).

orbitals of highest energy (from LUMO+1 to LUMO+9, only LUMO+1 is shown in Fig. 7), and the protonation of this molecule leads to an important decrease in energy of the π^* antibonding orbitals involving the C=O group. From these considerations we can propose that the important red shift observed in α-crustacyanin can be produced not only from a change in the ground electronic state conformation (demonstrated from the Raman spectra that is a property of the ground electronic state) but also from an interaction in the excited electronic state that significantly decreases the energy of the antibonding orbitals on the C=O group. The energy difference between the ground and excited electronic state decreases and can lead to a large bathochromic shift. In a protein the antibonding orbitals may also shift because of electrostatic interactions with the binding pocket of the protein. This model in which both ground and excited electronic states are perturbed upon binding can also explain why the correlation between ν_1 (property of the ground state) and $1/\lambda_{max}$ (property of both the ground and excited electronic states) is different for carotenoids and astaxanthin proteins.[4,15,17] The geometry of the orbitals of models in which the associated positive charge stabilized with a water molecule in a hydrogen bonding position (structure V and VI) were calculated and the shapes were not modified, we obtained only a small decrease of the energies.

For the monoprotonated molecule (structure III), which was considered as a possible model for the bathochromic shift, the CI calculation indicates that the transition with the largest oscillator strength (calculated at 767 nm) is a mixing of the HOMO $\rightarrow$ LUMO and the HOMO-1 $\rightarrow$ LUMO configurations with respective CI coefficients of 0.330 and 0.362. The scheme of the involved orbitals (Fig. 8) indicates that the ground state is significantly perturbed (from the geometry of the HOMO and HOMO-1), and the great asymmetry of the conjugated system is evident. However, as mentioned above, the RR results are consistent with a moderate modification of the conformation of the ground electronic state, and the studies performed by ^{13}C-MAS NMR show that the main perturbation is symmetrical in origin. This monoprotonated molecule cannot be considered as a valid model.
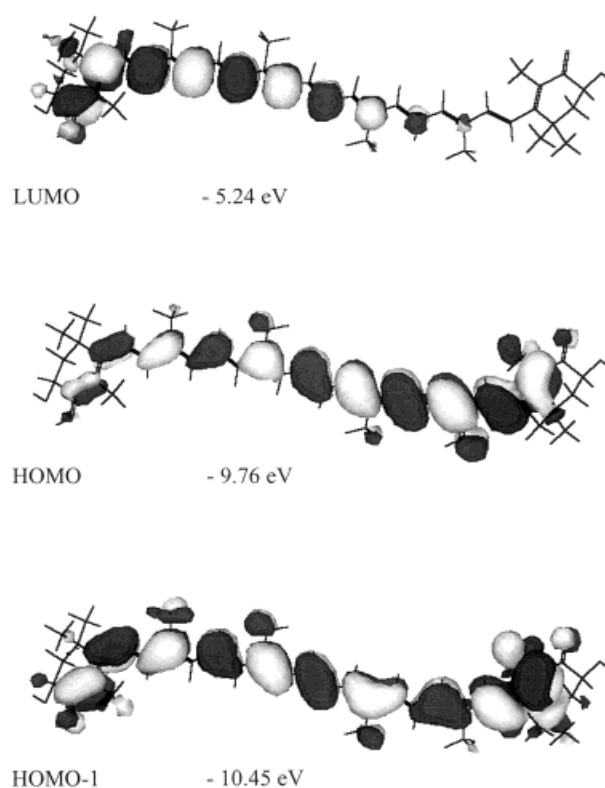

LUMO   – 5.24 eV

HOMO   – 9.76 eV

HOMO-1   – 10.45 eV

Figure 8. A schematic representation of the orbitals involved in the optical transition of monoprotonated astaxanthin (structure III).

CONCLUSIONS

From this study it appears that the interactions between astaxanthin and protein in α-crustacyanin decrease the energies of both the ground and excited electronic states.

The Raman data of the different ^{13}C-labeled astaxanthins, both free and bound to α-crustacyanin, provide additional support for an electron polarization mechanism. They show that the degree of delocalization of the π-electron system of the polyene chain is increased upon protein binding, which is expressed in a downward shift of the ν_1 line. Changes in the 1250–1400 cm^{-1} spectral range indicate that the geometry of the astaxanthin polyene chain is changed upon binding to the protein, although the absence of hydrogen out of plane modes argues against a large distortion.

Moreover, quantum chemical modeling studies reject the distortion mechanism as the sole effect responsible for the bathochromic shift of protein-bound astaxanthin. A correlation of the experimental data with the theoretical calculations supports a protonation mechanism of both asta-

xanthin ketofunctionalities as a possible model to account for the bathochromic shift. The stabilization by water molecules in a complex counterion may thus be considered for driving the protonation process. This result is in close agreement with the results of previous solid-state MAS NMR spectroscopy.

The analysis of the electronic energy levels and the geometry of the molecular orbitals involved in the optical transition of the doubly protonated astaxanthin suggest that the protonation of keto groups significantly decreases the energy of the $C=O$ antibonding orbitals that can thus participate more efficiently in the LUMO of the astaxanthin molecule in α-crustacyanin, and thus leads to a significant decrease of the energy gap between the ground and first excited electronic states.

REFERENCES

1. Britton, G.; Weesie, R. J.; Askin, D.; Warburton, J. D.; Gallardo–Guerrero, L.; Jansen, F. J. H. M.; de Groot, H. J. M.; Lugtenburg, J.; Cornard, J. P.; Merlin, J. C. Pure Appl Chem 1997, 69, 2075–2084.

2. Zagalsky, P. F.; Eliopoulos, E. E.; Findlay, J. B. C. Comput Biochem Physiol 1990, 97B, 1–18.

3. Buchwald, M.; Jencks, W. P. Biochemistry 1968, 7, 844–859.

4. Salares, V. R.; Young, N. M.; Bernstein, H. J.; Carey, P. R. Biochim Biophys Acta 1979, 576, 176–191.

5. Weesie, R. J.; Askin, D.; Jansen, F. J. H. M.; de Groot, H. J. M.; Lugtenburg, J.; Britton, G. FEBS Lett 1995, 362, 34–38.

6. Weesie, R. J.; Jansen, F. J. H. M.; Merlin, J. C.; Lugtenburg, J.; Britton, G.; de Groot, H. J. M. Biochemistry 1997, 36, 7288–7296.

7. Weesie, R. J.; Merlin, J. C.; Lugtenburg, J.; Britton, G.; Jansen, F. J. H. M.; Cornard, J. P. Biospectroscopy 1999, 5, 19–33.

8. Zagalsky, P. F. Methods Enzymol 1985, 111B, 216–247.

9. Zagalsky, P. F.; Clark, R. J. H.; Fairclough, D. P. Comput Biochem Physiol 1983, 75B, 169–170.

10. Jansen, F. J. H. M.; Kwestro, M.; Schmitt, D.; Lugtenburg, J. Recl Trav Chim Pays-Bas 1994, 113, 552–562.

11. Gajewski, J. J.; Gilbert, K. E. The MMX Method; CADCOM International Package: Gennevilliers, France.

12. Dewar, M. J. S.; Zoebisch, E. G.; Healy, E. F.; Stewart, J. J. P. J Am Chem Soc 1985, 107, 3902–3909.

13. Hypercube, Inc.: Gainesville, FL.

14. Salares, V. R.; Young, N. M.; Bernstein H. J.; Carey, P. R. Biochemistry 1977, 16, 4751–4756.

15. Clark, R. J. H.; D'Urso, N. R.; Zagalsky, P. F. J Am Chem Soc 1980, 102, 6693–6698.

16. Merlin, J. C.; Thomas, E. W.; Shone, C. C.; Britton, G. Biochim Biophys Acta 1987, 913, 111–116.

17. Merlin, J. C. J Raman Spectrosc 1987, 18, 519–523.

18. Zagalsky, P. F.; Gilchrist, B. M.; Clark, R. J. H.; Fairclough, D. P. Comp Biochem Physiol 1983, B74, 647–660.

19. Warburton, J. Ph.D. Thesis, University of Liverpool, Liverpool, U.K., 1986.

20. Weesie, R. J. Ph.D. Thesis, University of Liverpool, Liverpool, U.K., 1996.

21. Saito, S.; Tasumi, M. J Raman Spectrosc 1983, 14, 310–321.

22. Rimai, L.; Heyde, M. E.; Gill, D. J Am Chem Soc 1971, 93, 6776–6780.

23. McRae, E. G.; Kasha, M. In Physical Processes in Radiation Biology; Augenstein, L., Ed.; Academic: New York, 1964; p 23.

24. Weesie, R. J.; Verel, R.; Jansen, F. J. H. M.; Britton, G.; Lugtenburg, J.; de Groot, H. J. M. Pure Appl Chem 1997, 69, 2085–2094.

25. Kofranek, M.; Lischka, H.; Karpfen, A. J Chem Phys 1992, 96, 982–996.